

Original Article

Rapid Enzymatically Reduction of Zincum Gluconicum for the Biomanufacturing of Zinc Oxide Nanoparticles by Mycoextracellular Filtrate of *Penicillium Digitatum* (Pdig-B3) as a Soft Green Technique

Issa, M. A. S^{1*}*1. Department of Biology, College of Sciences, University of Thi-Qar, Nasiriyah, Iraq*Received 2 October 2021; Accepted 29 October 2021
Corresponding Author: mohammed1971_issa@sci.utq.edu.iq**Abstract**

Molds have been used as micro-biofactories for biomanufacturing of metal oxide nanoparticles (MetNps) since they are effortless, immaculate, safe, non-poisonous, vital-biocompatible, and environmentally acceptable. The present study aimed to explore the bioindustry, mold screening protocol, and characterization of zinc oxide nanoparticles (ZnONPs) using a diverse filamentous Green mold (FiGM) isolated from spoiled citrus fruits. Eight filamentous *Penicillium digitatum* mold strains had been obtained and subjected to investigate the capability of ZnONPs biosynthesis by fungal extracellular free-cell filtrate. *P. digitatum* (P-digB3) obtained the peak of ZnONPs (379 nm) detected by the UV-visible spectrophotometry and was found as a significantly optimum strain in the highest quantity (mean±SD: 0.0138±0.001 gm/100 ml) and the smallest average NPs size. The ZnONPs were characterized by UV-visible scanning spectrophotometry, Atomic Force Microscopy, X-RD, Scanning Electron Microscopy (SEM), and Transmission Electron Microscopy (TEM). The final average size of ZnONPs was obtained at 65.46 nm with diversified shapes and dimensions. The present study concluded the high capabilities of fungi (FiGMs) as eco-friendly and cheap bio-nano factories to manufacture ZnONPs with great nano-level average size, which may consider new boost sources for use in many nano-sectors and applications.

Keywords: *P. digitatum* (Pdig-B3), SEM and TEM, Zincum gluconicum, ZnONPs**1. Introduction**

In the contemporary period, ennobling of metal nanoparticles (MeNps) is correlated with very small particle sizes ranging from 1 to preferable less than 100 nm. Due to their extremely small size and high surface area to volume ratio, MeNps exhibit distinctive properties, which have been attributed to substantial variations in properties over their bulk counterparts. In this respect, by offering advanced technologies, NPs have been incorporated into numerous industrial sectors (1), which have been vastly used in photonics, microelectronics,

information storage, catalysts, energy conversion, and communications (2), as well as medicinal applications (vaccines and drugs) (3).

Due to their unusual properties as a semi-conductor submitting an elevated band gap of 3.4 eV and binding energy of 60 meV leading to peculiar electrical and optical properties (4), zinc oxide nanoparticles (ZnONps) have gained considerable popularity in modern years. In fact, research has demonstrated that zinc in living organisms is an essential nutrient. As such, microbial cells or enzymes, proteins, and other biomolecules are used

for the synthesis of ZnONPs by both prokaryotes and eukaryotes, including bacteria, fungi, and yeast. ZnONPs exhibit antimicrobial properties; however, the properties of NPs are depended upon their size and shape, which make them specific for various applications (1).

The biological approach was applied with the aid of using the biologically energetic products of bacteria, fungi, plants, and yeasts reflecting the excellent sources for the production of NPs. Mostly, fungi were chosen instead of bacteria because of their immovability, better metal bioaccumulation capacity, and high-binding efficiency. There are numerous applications of fungi as they produce huge enzymes and are simple in the scale-up operation, cost-effective, and easy in handling the biomass (5). Hefny, El-Zamek (6) used the culture filtrates of diverse species of *Aspergillus*, *Fusarium*, and *Penicillium* biosynthesis ZnONPs. Moreover, *Aspergillus parasiticus* (Ap4) and *Penicillium italicum* were exploited by Issa, Al-Sheikhly (7), as well as Taha, Howar (8) for the bio-fabrication of ZnONPs and silver (Ag) Nps, respectively.

Penicillium digitatum defined as filamentous green mold is one of the significant causes of post-harvest citrus rot and has diversified intra-extracellular reducing enzymes. Since there is not enough research about this species regarding NPs biosynthesis, this study as the first attempt aimed to investigate the *P. digitatum* filtrate efficacy in reducing zinc gluconate hydrate as a source in biomanufacturing of ZnONPs as a simplified, zero-cost, and eco-friendly route.

2. Materials and Methods

2.1. Chemicals

Zincum gluconate hydrate (C₁₂H₂₂O₁₄Zn) (Analar, England), potato dextrose agar (PDA), malt extract, peptone, agar (Himedia, India), glucose, NaOH, HCl, chloramphenicol (BDH, England), KH₂PO₄ and K₂HPO₄ (CDH, India), MgSO₄.7H₂O, and (NH₄)₂SO₄ (Merek, Germany) were utilized in this study. Moreover, this study employed the analytical grade of all chemicals and reagents.

2.2. Filamentous Green Mold Isolation

Infected citrus fruits, including citrus reticulata (Mandarin), orange (*Citrus aurantium*), lemon (*Citrus limon*), citrus maxima (Pomelo), and bitter orange (*Citrus amara*) were purchased from a local market with spoiled status morphology. After that, the surface was sterilized with cotton soaked in ethanol 70%. They were then cut out into small segments (1½-1½cm) using a sterilized scalpel. Next, the segments (three on each plate) of the infected samples were plated on solidified PDA(10 gm/250 ml) supplemented with chloramphenicol (25 mg/250 ml) (9). Inoculated plates were incubated at 28±1 °C for five-seven days. From the incubated plates, different fungal isolates with different colorations were observed that especially included Green or Blue-Grey which signified that the target was approximately *Penicillium* genus. The fungal colonies that emerged were continuously sub-cultured (picked from the edge of an advancing colony with a sterile fine-tipped needle) in order to obtain a pure culture of the fungal isolates. The pure isolated fungi were maintained on PDA slants and refrigerated at 4 °C for further studies (10).

2.3. Identification of Pure Filamentous Green Mold Isolates

The identical pure isolated fungi were identified and diagnosed at the Central Fungi Laboratory of Postgraduate, Faculty of Sciences, University of Basra, Basra, Iraq, according to the most recent protocols and documented keys in fungal identification (11, 12). The filamentous green mold (FiGM) isolates were subjected to certain morphological observation, as well as microscopical studies. All fungal strains were maintained in slants (universal glass tube) with two replicates each on the MGPA composed of 2% g/l malt extract, 2% g/l glucose, 0.1% g/l peptone, and 1.5% g/l agar as stock cultures at 4-8 °C. These are periodically reactivated by regular subculturing (13).

2.4. Filamentous Green Mold Biomass and Active Mycofiltrate Preparation

One batch rocking aerobically submerged fermentation (Obr-Smf) in 250 ml Erlenmeyer flasks

(Em.f) had been used to produce FiGM biomass in 100 ml base fortified malt extract peptone glucose liquid media at specific incubation parameters until obtaining the reducing active broth used for the biosynthesis of ZnONPs according to a study by Issa, Al-Sheikhly (7).

2.5. Zinc Gluconate Hydrate Reducing to Zinc Oxide Nanoparticle by Mycofiltrate

About 50 ml of one and a half mole zinc gluconate hydrate (dissolved 341.775 mg $C_{12}H_{22}O_{14}Zn$ in 500 ml deionized distilled water [d.s.d.w]) solution of the final concentration was mixed with 50 ml of activation fungal filtrate in an Em.f.

Two flasks (250 ml and adjusted pH=7.0) were added, one with mycofiltrate (without $C_{12}H_{22}O_{14}Zn$) and the other with only pure zinc gluconate solution (free-mycofiltrate) as positive and negative controls, respectively. They were then incubated in an orbital shaker incubator with 140 jolts per min at 30°C for three days in triplicate (7).

When the deposition of white precipitate was started to occur at the bottom of the flask, it was indicated that the transformation process had been achieved and produced ZnONPs, which helped to detect which of the strains were successful in ZnONPs fabrication, followed by the washed of accumulation thoroughly with d.s.d.w to remove all the ions and other impurities through filtering by Whatman (No.1) paper, followed by 0.45 μm Millipore filter under reverse vacuum pressure for excess purity (14).

The white aggregate formed at the flask base was separated from the filtrate by centrifugation (15 ml centrifuge tubes) twice at 10,000 $\times g$ for 15 min with 5-min intervals. Finally, the milky-white precipitate was drying in a vacuum oven at 105°C. After that, the harvested fine powder of ZnONPs had been weighed for the next experiments (15).

2.6. Election of the Superior Strain in the Manufacturing of ZnONPs

To screen the preferable fungal strains which have the capability to fabricate ZnONPs at both quantity and quality levels, the selection had been achieved, firstly,

upon their ability to form the misty and turbidity in the bioreactor reaction of mycelial aqueous extract in the inception. Subsequently, 2 ml of partial hazy solution was subjected to the UV-vis spectral analysis conforming with wave length according to standard references between 340 and 390 nm. Thirdly, the white precipitations deposited at the bottom of the bioreactor flask indicated the ability of the fungal strain to synthesis of ZnONPs confirmatively and quantitatively (13). In addition, the smallest particles in both diameter and average size detected by Atomic Force Microscope (AFM) as qualitatively screening both parameters restricted the best isolate for more studies in NPs manufacturing field (16).

2.7. Characterization of Zinc Oxide Nanoparticles of Final Production

2.7.1. X-Ray Diffraction

The structural characterization was analyzed in order to obtain information about particle size, crystal structure, and surface morphology using X-Ray Diffraction at the Central Service Laboratory, Faculty of Education for Pure Sciences, Ibn Al-Haitham University, Baghdad, Iraq, by a diffractometer recorded in the range of $20 \leq 2\theta \leq 90$ angles and using Cu-K α as an anode. The average crystallite size can be calculated using Debye-Scherrer Equation (17).

$$D_{hkl} = k \lambda \times \beta_{hkl} \times \cos \theta_{hkl} \dots \dots \dots (1)$$

Where D_{hkl} is the mean size of the ordered (crystalline) domains, hkl signifies the Miller indices of the planes being analyzed, $K=0.88-0.9$ presents the Scherrer equation, λ indicates the X-ray wavelength, β is the line broadening at half the maximum intensity [FWHM], and θ presents the Bragg angle.

2.7.2. SEM and TEM Imagination Studies

Via Electronic Scanning Microscopy (SEM-112544/Angstrom Advanced-USA) to record the micrograph images of synthesized ZnONPs and investigate the homogeneity of the nano-powder, the surface of the prepared and annealed ZnO nano-powders had been scanned in the SEM-Unit at the Ministry of Science and Technology/Materials,

Research Department, Iraq. Furthermore, to measure and confirm the dimensional nanostructures of the ZnONPs powders' architectural morphology manufactured by different FiGM isolates by transmission electron microscope (TEM) (CM10/Philips, Holland), the measurements were provided with carbon-coated copper specimen holder grids. TEM micrographs were taken using a low voltage (100 kV) in the Technograph Unit of TEM at the Faculty of Medicine, Al-Nahrain University, Iraq.

2.8. Statistical Analysis

All experiments were conducted in triplicate, and the results were presented as mean±SD or SE (standard division and error, respectively). The Ready Statistical Analysis IBM-SPSS software (version 22) was used to detect the differences among means with the Post-hoc-Tukey/ALPHA ($\alpha=0.01$) test through the analysis of variance (One-way ANOVA), and $P<0.01$ was considered statistically significant.

3. Results and Discussion

3.1. Identification FGMS Isolates

The effort of collection manifested and targeted to eight isolates of *P. digitatum* from various citrus fruits is sorted in table 1.

Table 1. Recovering process outcomes and number of *P. digitatum* from different citrus fruits

Source of Isolation		Total
Pdig-M1 Pdig-M2	<i>Citrus reticulata</i> (Mandarin)	2
Pdig-B3	<i>Citrus amara</i> (Bitter orange)	1
Pdig-P4	<i>Citrus maxima</i> (Pomelo)	1
Pdig-L5 Pdig-L6	<i>Citrus limon</i> (Lemon)	2
Pdig-O7 Pdig-O8	<i>Citrus aurantium</i> (Orang)	2

The collection of the rotten citrus fruits took the first 10 days of November in 2020, and the study deliberately targeted the isolates of the fungus *P. digitatum* (greenish-olive rot) from citrus fruits shown in figure 1 and neglecting the rest of the species by

relying on the phenotypes that include the shape and colour of the fungus yarn in addition to the growth velocity, and the area occupied by the colony in the culture dish in 96 h on different culture media. The microscopic examinations included staining with the lactophenol cotton blue dye to show the accurate structures and measure them (conidiophores, large phialides, and conidia). The cones of spores, the dimensions, as well as the shapes of their surfaces and their edges, are enough to reach the diagnostic goal which was in line with the results of a study conducted by Taha, Howar (8) when *P. italicum* was isolated and diagnosed from the Iraqi citrus lemon.

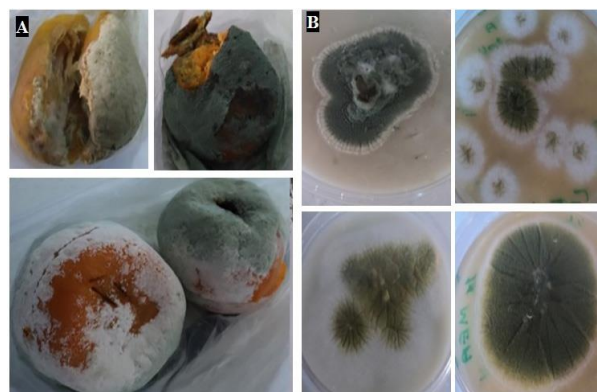


Figure 1. Various rotten citrus fruits as a source of the isolation of FiGms (A). Different Pure cultures of *Penicillium digitatum* isolates (B).

3.2. Fabrication and Characterization of Myco-ZnONPs by Mycofiltrate of FiGMS

The analysis of UV-visible shows the peaks and formation of hazy filtrate with white-milky precipitation. The first detection among FiGM isolates had been performed to select the strains which could be able to reduce $C_{12}H_{22}O_{14}Zn$ to ZnONPs. The results in table 2 show that all *P. digitatum* isolates were given the compatible peaks with a range of ZnONPs (320-390 nm); however, only Pdig-B3, Pdig-L5, Pdig-L6, and Pdig-O7 were able to form the foggy status in filtrate reaction, and finally, the white-milky nanopowder had been deposited (Figure 2). Some strains were given ZnONPs peak; however, they could not be able to appear in the misty form, and they deposited in the form of white powder as in Pdig-M1. On the other

hand, others obtained the foggy white colour; however, they were unable to precipitate nano-powder as in Pdig-M2, Pdig-P4, and Pdig-O8 which incapacitate to fabricate ZnONPs. These results are compatible with the findings of a study conducted by Chauhan, Reddy (18) who synthesized the wavelength of ZnONPs by yeast *Pichia fermentans* JA2 at 374 nm. However, the results of this study were not in line with the wavelength peak of ZnONPs manufactured by

Aspergillus terreus in a study by Baskar, Chandhuru (15) that was 340 nm. The variations in the diversity scope capability of ZnONPs among fungal strains in the recent study can be due to several reasons, including sources of isolation, diversity and adaptation growth of microorganism (fungi) strains (19), potential to utilize substrate and nutrients in bioreactor culture, and biomolecules responsible for biosyntheses, such as NADH, NADPH, and FAD (20).

Table 2. Sifting of an optimum isolate of *P. digitatum* capable of ZnONPs bio-fabrication

FiGM strains	Mean±SD of the position peak (nm)	Mistiness formation	Presence of white precipitate	Mean of Sum (gm/100 ml)±SD	†Mean size by AFM (nm)±SE
Pdig-M1	349±1.4	-	-	-	-
Pdig-M2	364±1.7	+	-	-	-
Pdig-B3	379±1.3	+	+	0.0138±0.001	66.91±1.46
Pdig-P4	373±2.6	+	-	-	-
Pdig-L5	378±2.3	+	+	0.0143±0.002	113.63±2.53
Pdig-L6	371±2.8	+	+	0.0064±0.001	154.48±3.24
Pdig-O7	367±1.7	+	+	0.0019±0.002	137.43±8.11
Pdig-O8	353±2.2	+	-	-	-

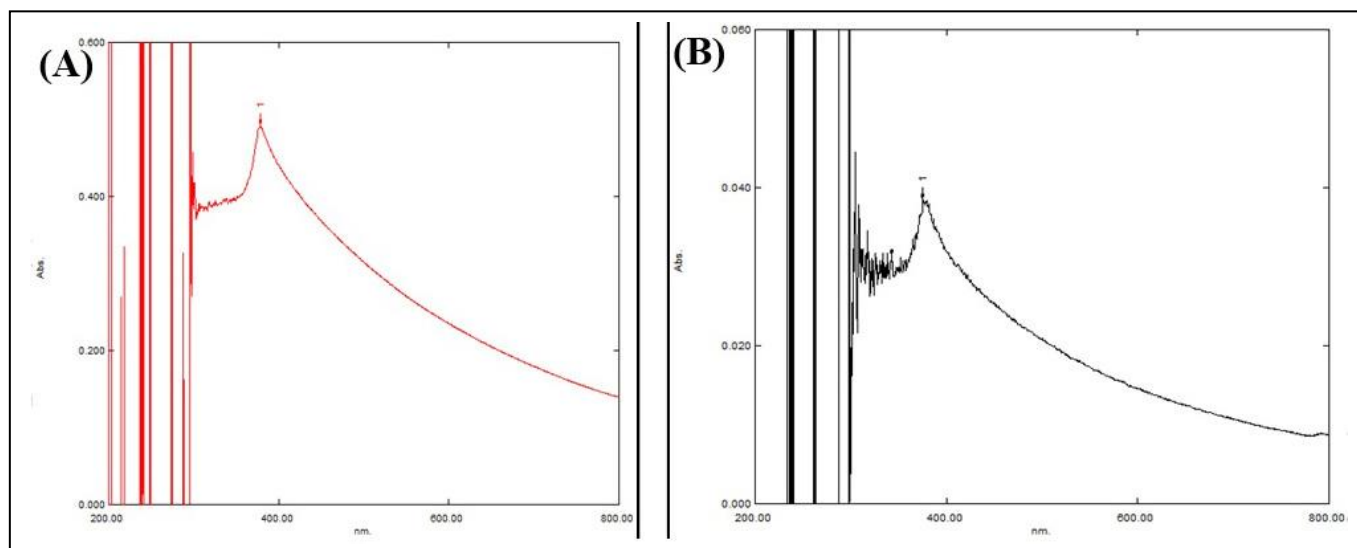


Figure 2. UV-visible peak plots in the first election of *Penicillium digitatum* Pdig-B3 (A) and Pdig-L5 (B)

More other results are shown in table 3 and figure 3 that show significant differences in the quantity of ZnONPs powder that is higher in Pdig-B3 and Pdig-L5, compared to Pdig-L6 and Pdig-O7. Although there are no significant differences between Pdig-B3 and Pdig-L5 in the amount of nano-powder, the average size of NPs was determined by AFM shown in figure 4. The

results showed highly significant differences and *P. digitatum* Pdig-B3 that obtained the smallest average size of NPs (with an average size of 67.37 nm) opposite to the rest of the isolates; therefore, Pdig-B3 was approximately more preferable one, compared to other isolates due to adequate good quantity production with an average size of a great nano-characteristic.

Table 3. The differences of mean weight (A), and the mean particle size (B) among *P. digitatum* isolates that capable to ZnONPs bio-fabrication

Tukey HSD ^a of Mean Weight (A)				
<i>P. digitatum</i> strains	N	Subset fir alpha = 0.01		
		1	2	3
Strain Pdg-o7	3	.0019		
Strain Pdg-16	3		.0064	
Strain Pdg-b3	3			.0138
Strain Pdg-15	3			.0143
Sig.		1.000	1.000	.901

Tukey HSD ^a Particles Size (B)				
<i>P. digitatum</i> strains	N	Subset fir alpha = 0.01		
		1	2	3
Strain Pdg-b3	3	67.3767		
Strain Pdg-15	3		107.7667	
Strain Pdg-o7	3		134.5600	134.5600
Strain Pdg-16	3			154.8867
Sig.		1.000	.011	.044

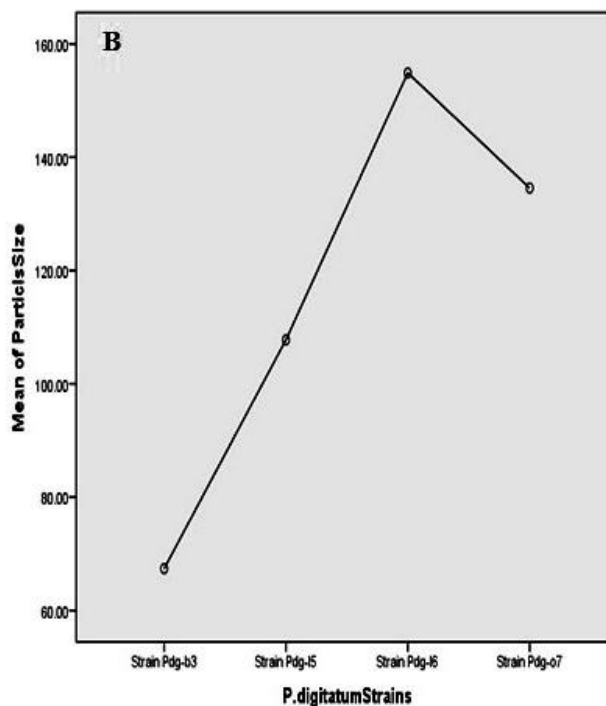
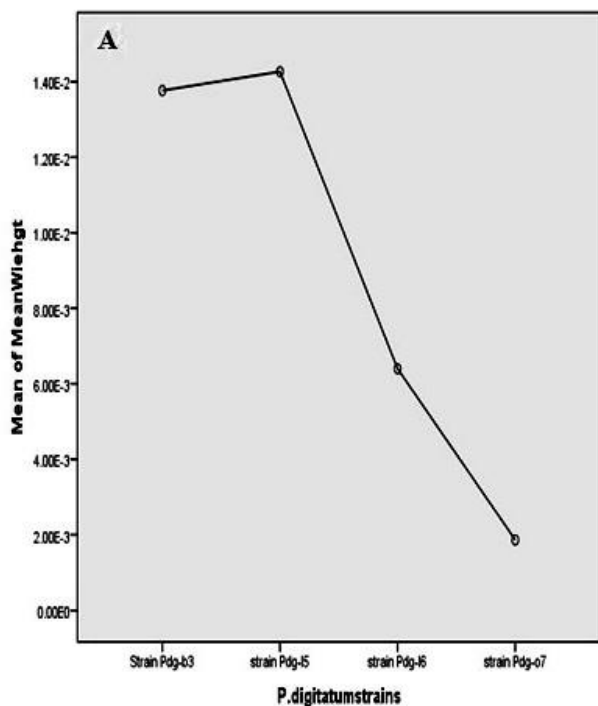


Figure 3. The differences plot of mean weight (A), and the mean particle size (B) among *P. digitatum* isolates that capable to ZnONPs bio-fabrication

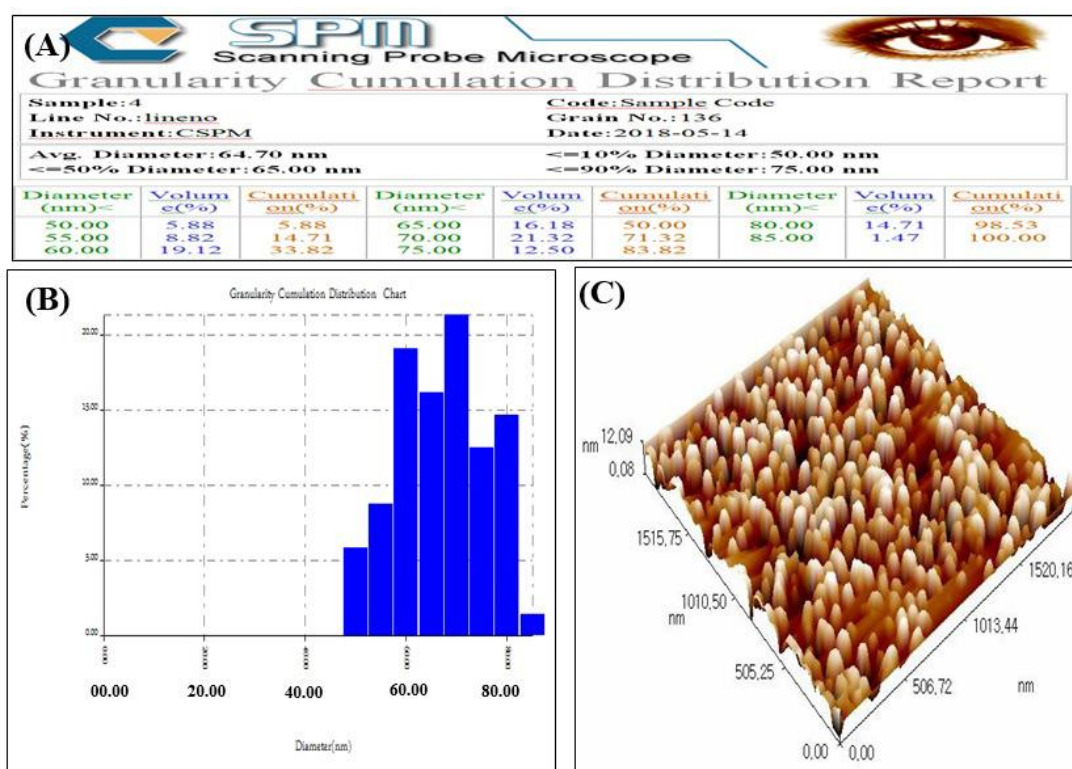


Figure 4. Distribution chart (A), Histogram (B), and Surface roughness analysis (C) of the ZnONPs manufactured by *Penicillin digitatum* (Pdig-B3) (one of the triplicate tests)

Accurate determination of the average size and crystallographic characteristics was performed using X-ray diffraction to substantiate various phases of ZnONPs. In figure 5, the standard wurtzite and XRD patterns of ZnONPs are depicted. The phase identification of ZnONPs was conducted using the X-ray powder diffraction (XRD) with 2θ ranges from 20° to 80° , 0.02° s⁻¹ of scanning rate and Cu $K\alpha$ radiation of 0.1540 nm. The XRD peaks at 31.7° , 34.91° , 36.3° , 47.53° , 56.61° , 67.96° , and 69.1° were identified as (1 0 0), (0 0 2), (1 0 1), (1 0 2), (1 1 0), (1 1 2), and (2 0 1), reflections, respectively. The product is found to have a fine crystalline structure as demonstrated by the sharper and stronger diffraction peaks. The average crystallite size of the isolate Pdig-B3 myco-ZnONPs was estimated by Scherrer's formula that found to be 63.46 nm.

3.3. Micrograph Image Analysis of Myco-ZnONPs by SEM and TEM

The confirmation of the final product of the ZnONPs morphology comes from the analysis of SEM and TEM

micrographs. The micrograph of SEM is illustrated in figure 6. On the other hand, TEM analysis shows a diversity in the geometrical crystalline shapes in the morphology of ZnONPs with an average size of 63 - 68 nm represented in figure 7. This result is consistent with the findings of a study conducted by Rajan, Cherian (14) who estimated the average of ZnONPs synthesis by *Aspergillus fumigatus* (JCF) at 60 - 75 nm the same as filamentous molds.

These results are somewhat close to the findings calculated by the X-ray diffraction analysis. Therefore, taking into account the values, plane faces, crystallo-diffractions, and topography images obtained from AFM, X-RD, SEM, and TEM, the final average size of the NPs manufactured by *P. digitatum* (Pdig-B3) at recent growth and biomanufacturing conditions will be approximately 65.46 nm. The resultant of the recent study was incompatible with the findings of a study conducted by Mashrai, Khanam (21) which detected the average sizes of ZnONPs

manufactured by *Candidia albicans* using SEM and TEM at 15-20 nm and ~ 20 nm, respectively, this may

be due to differences in the type of microorganism utilization.

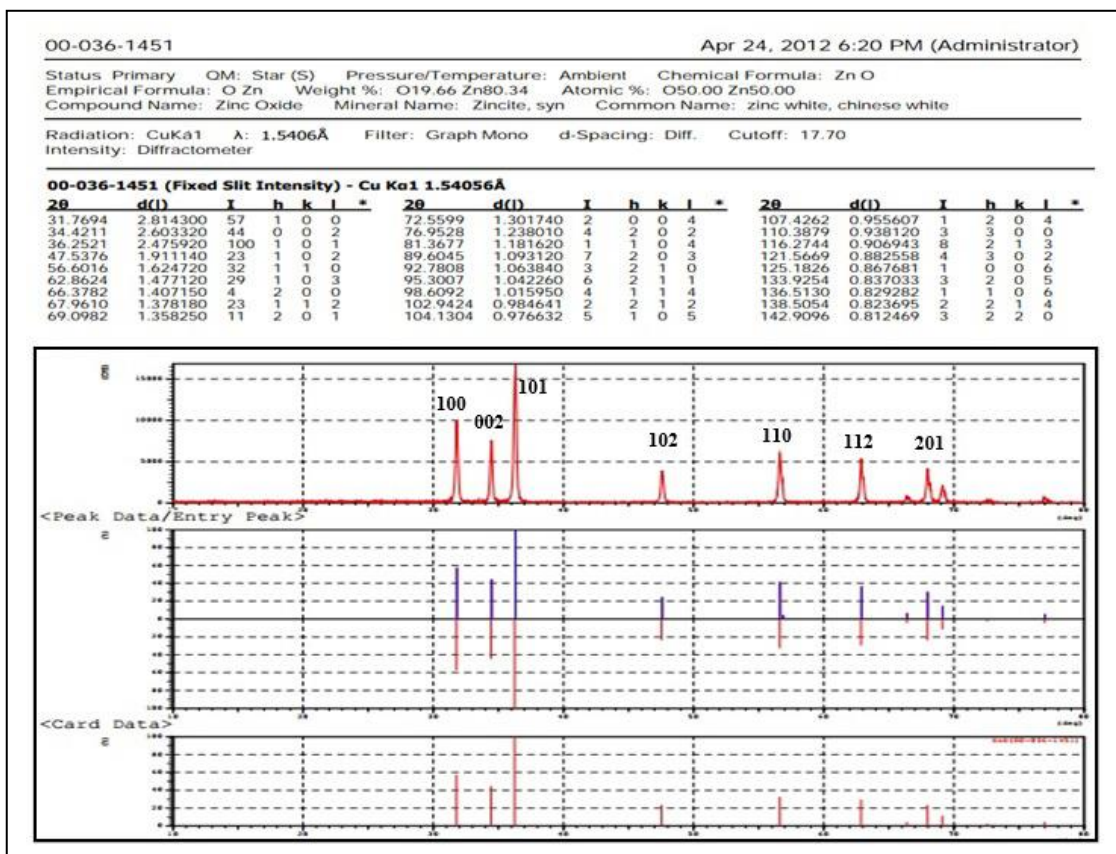


Figure 5. XRD pattern of biosynthesized ZnONPs by extracellular free cells filtrate by *P. digitatum* Pdg-b3

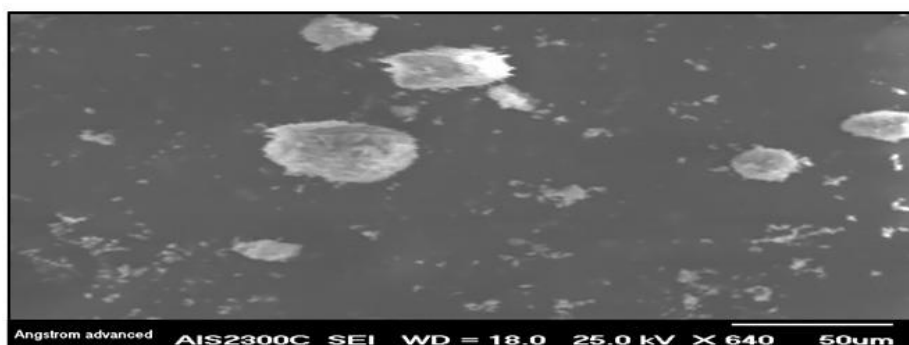


Figure 6. SEM image of ZnONPs mycosynthesis by *P. digitatum* (Pdig-B3)

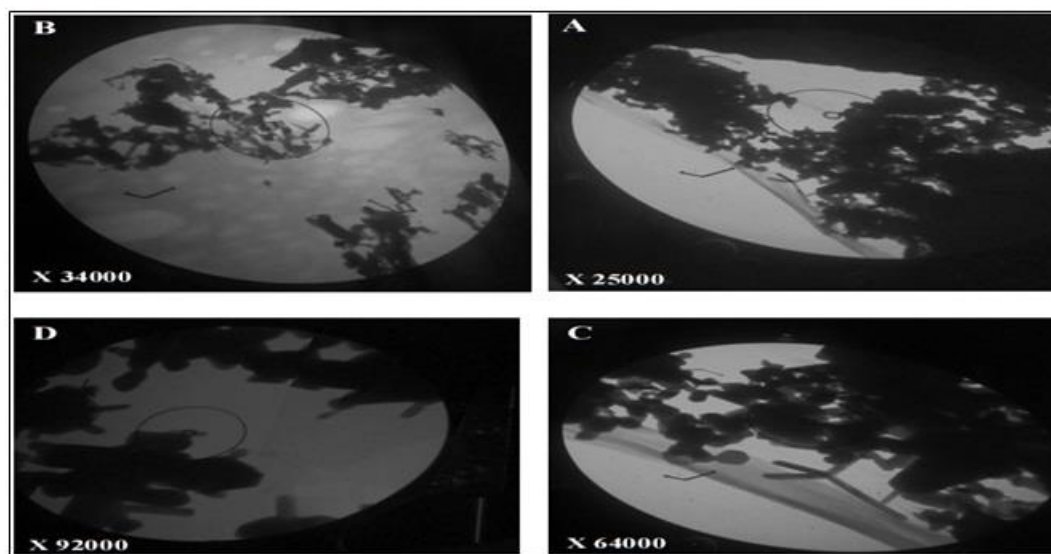


Figure 7. TEM images of different shapes of ZnONPs manufactured by *P. digitatum* (Pdigi-B3), A=25000 \times , B=34000 \times , C=64000 \times , and D=92000 \times

The current study is the first regional report in its content on the use of *P. digitatum* in bio-synthesis of ZnONPs which concluded that the extracellular reduction by free-cell filtrate of *P. digitatum* (Pdigi-B3) was the best among other FiGM strains which were isolated from citrus fruits of extremely low pH. Moreover, it was shown as a convenient protocol to fabricate ZnONPs by the reduction of zinc gluconate hydrate, which had been characterized via different combination complementary mechanization and devices including UV-visible, AFM, X-RD, SEM, and TEM. The approach provides an eco-friendly, simple scaling-up, cheap, and efficient route for the biomanufacturing of well-structured shaped ZnONPs that give many expansions in nano-implementations and participation of diverse fields.

Authors' Contribution

Study concept and design: M. A. S. I.

Acquisition of data: M. A. S. I.

Analysis and interpretation of data: M. A. S. I.

Drafting of the manuscript: M. A. S. I.

Critical revision of the manuscript for important intellectual content: M. A. S. I.

Statistical analysis: M. A. S. I.

Administrative, technical, and material support: M. A. S. I.

Conflict of Interest

The authors declare that they have no conflict of interest.

Grant Support

This study was carried out using personal support without any financial support from any university, academic, scientific, or commercial institution.

Acknowledgment

The author would like to express gratitude to the University of Thi-Qar, Faculty of Sciences, Faculty of Medicine, Al-Nahrain University, Iraq, and the Central Fungi Laboratory of Postgraduate, Faculty of Sciences, University of Basra, Iraq, for being supportive and helpful to complete this novel project.

References

1. Yusof HM, Mohamad R, Zaidan UH. Microbial synthesis of zinc oxide nanoparticles and their potential application as an antimicrobial agent and a feed supplement in animal industry: a review. *J Anim Sci Biotechnol.*

- 2019;10(1):1-22.
2. Li H, Yan S, Deng C, Dou S, Ren X, editors. Synthesis and characterization of Ag nanoflowers with different morphologies. IOP Conference Series: Materials Science and Engineering; 2021: IOP Publishing.
 3. Kareem S, Jarullah BA. Improvement of Newcastle disease virus vaccine by using gold nanoparticles and some natural food additives. *Univ Thi-Qar J Sci.* 2017;6(2):59-64.
 4. da Silva BL, Abuçafy MP, Manaia EB, Junior JAO, Chiari-Andréo BG, Pietro RCR, et al. Relationship between structure and antimicrobial activity of zinc oxide nanoparticles: An overview. *Int J Nanomedicine.* 2019;14:9395.
 5. Kalpana V, Kataru BAS, Sravani N, Vigneshwari T, Panneerselvam A, Rajeswari VD. Biosynthesis of zinc oxide nanoparticles using culture filtrates of *Aspergillus niger*: Antimicrobial textiles and dye degradation studies. *OpenNano.* 2018;3:48-55.
 6. Hefny ME, El-Zamek FI, El-Fattah A, Mahgoub S. Biosynthesis of Zinc Nanoparticles Using Culture Filtrates of *Aspergillus*, *Fusarium* and *Penicillium* Fungal Species and Their Antibacterial Properties against Gram-Positive and Gram-Negative Bacteria. *Zagazig J Agric Res.* 2019;46(6):2009-21.
 7. Issa MA, Al-Sheikhly AA, Hamid MK, Nader M. Novel rapid green fabrication of ZnO nps using mycofiltrate by local fungus *Aspergillus Parasiticus* Ap4. *Biosci Res.* 2018;15(3):2159-70.
 8. Taha ZK, Howar SN, Sulaiman GM. Isolation and identification of *Penicillium italicum* from Iraqi citrus lemon fruits and its ability manufacture of silver nanoparticles and their antibacterial and antifungal activity. *Res J Pharm Technol.* 2019;12(3):1320-6.
 9. Elfita E, Muharni M, Yohandini H, Fadhilah F, editors. Antioxidant activity of endophytic fungi isolated from the stem bark of *Swietenia mahagoni* (L.) Jacq. IOP Conference Series: Materials Science and Engineering; 2021: IOP Publishing.
 10. Sri V, Rajagopal K. Isolation and Identification of Thermo Tolerant Endophytic Fungi from *Melia dubia* and Synthesis of Zinc Nano Particles. *J. Nanosci Nanotechnol.* 2016;7(2):99-112.
 11. Pitt JI, Hocking AD. *Fungi and food spoilage*: Springer; 2009.
 12. Visagie C, Houbraeken J, Frisvad JC, Hong S-B, Klaassen C, Perrone G, et al. Identification and nomenclature of the genus *Penicillium*. *Stud Mycol.* 2014;78:343-71.
 13. Ottoni CA, Simões MF, Fernandes S, Dos Santos JG, Da Silva ES, de Souza RFB, et al. Screening of filamentous fungi for antimicrobial silver nanoparticles synthesis. *AMB Express.* 2017;7(1):1-10.
 14. Rajan A, Cherian E, Baskar G. Biosynthesis of zinc oxide nanoparticles using *Aspergillus fumigatus* JCF and its antibacterial activity. *Int J Mod Sci Technol.* 2016;1:52-7.
 15. Baskar G, Chandhuru J, Fahad KS, Praveen A. Mycological synthesis, characterization and antifungal activity of zinc oxide nanoparticles. *Asian J Pharm Technol.* 2013;3(4):142-6.
 16. Mahmood S, Mandal UK. Morphological characterization of lipid structured nanoparticles by atomic force microscopy while minimizing the formation of failed artefacts. *Curr Nanosci.* 2017;2(1):24-32.
 17. Bayroodi E, Jalal R. Modulation of antibiotic resistance in *Pseudomonas aeruginosa* by ZnO nanoparticles. *Iran J Microbiol.* 2016;8(2):85.
 18. Chauhan R, Reddy A, Abraham J. Biosynthesis of silver and zinc oxide nanoparticles using *Pichia fermentans* JA2 and their antimicrobial property. *Appl Nanosci.* 2015;5(1):63-71.
 19. Singh P, Kim Y-J, Zhang D, Yang D-C. Biological synthesis of nanoparticles from plants and microorganisms. *Trends Biotechnol.* 2016;34(7):588-99.
 20. Khandel P, Shahi SK. Microbes mediated synthesis of metal nanoparticles: current status and future prospects. *Int J Nanomater Biostruct.* 2016;6(1):1-24.
 21. Mashrai A, Khanam H, Aljawfi RN. Biological synthesis of ZnO nanoparticles using *C. albicans* and studying their catalytic performance in the synthesis of steroidal pyrazolines. *Arab J Chem.* 2017;10:S1530-S6.